J Pharmacol Sci **119**, 82 – 90 (2012)

Journal of Pharmacological Sciences

Full Paper

N- and L-Type Voltage-Dependent Ca^{2+} Channels Contribute to the Generation of After-Discharges in the Spinal Ventral Root After Cessation of Noxious Mechanical Stimulation

Shohei Yamamoto[1], Mitsuo Tanabe[2], and Hideki Ono[1,*]

[1]*Laboratory of CNS Pharmacology, Graduate School of Pharmaceutical Sciences, Nagoya City University, 3-1 Tanabe-dori, Mizuho-ku, Nagoya 467-8603, Japan*
[2]*Laboratory of Pharmacology, School of Pharmacy, Kitasato University, 5-9-1 Shirokane, Minato-ku, Tokyo 108-8641, Japan*

Received February 8, 2012; Accepted March 25, 2012

Abstract. Voltage-dependent Ca^{2+} channels (VDCCs) play a crucial role in the spinal pain transduction. We previously reported that nociceptive mechanical stimuli to the rat hindpaw evoked two types of ventral root discharges that increased during stimulation (during-discharges) and after cessation of stimulation (after-discharges). To explore the involvement of VDCCs in these ventral root discharges, several VDCC blockers were applied directly to the surface of the spinal cord. Spinalized rats were laminectomized. The fifth lumbar ventral root was sectioned and used for multi-unit efferent discharges recording. An agar pool was constructed on the first lumbar vertebra for drug application. Ethosuximide (a T-type VDCC blocker) had no effect on ventral root discharges. ω-Conotoxin GVIA (an N-type VDCC blocker) preferentially suppressed after-discharges. ω-Agatoxin IVA (a P/Q-type VDCC blocker), diltiazem, and verapamil (L-type VDCC blockers) nonselectively depressed both during- and after-discharges. The more selective L-type VDCC blocker nicardipine depressed only after-discharges and the depression was exhibited when nicardipine was microinjected into the dorsal horn, but not into the ventral horn. These findings suggested that N- and L-type VDCCs in the dorsal horn were involved in the generation of after-discharges and these blockers might be useful for treatment of persistent pain that involves the spinal pathway.

Keywords: after-discharges, dorsal horn, L-type voltage-dependent Ca^{2+} channel, N-type voltage-dependent Ca^{2+} channel, spinal cord

Introduction

Voltage-dependent Ca^{2+} channels (VDCCs) enable calcium ions to enter neurons upon depolarization and are thereby involved in neuronal functions such as release of neurotransmitters from presynaptic terminals and excitability of postsynaptic membranes. Generally, VDCCs are divided into L, N, P/Q, R, and T types on the basis of their electrophysiological and pharmacological properties (1). These channels play a crucial role in spinal neurotransmission involved in pain perception (2 – 4).

*Corresponding author. hiono@phar.nagoya-cu.ac.jp
Published online in J-STAGE on April 28, 2012 (in advance)
doi: 10.1254/jphs.12035FP

N-type and P/Q-type VDCCs are expressed specifically in the nervous system. N-type VDCCs are well established mediators of pain signals (5, 6), and N-type VDCC-KO mice show a reduced response to noxious stimuli through the reflex arc without any resulting abnormal motor behavior (7). N-type VDCCs exist in primary afferent fiber terminals mainly in the dorsal horn (6) and play an extremely important role in neurotransmitter release from primary afferent fibers (8, 9). The selective N-type VDCC-blocker ziconotide is used as an analgesic agent (10) because of its inhibitory effect on neurotransmitter release (11, 12). T-type and P/Q-type VDCCs are also involved in pain transmission. $Ca_V3.2$ T-type VDCCs contribute to the pro-nociceptive effects of hydrogen sulfide in the spinal cord as well as in pe-

ripheral tissues (13). Ethosuximide, a T-type VDCC blocker, displays an antinociceptive effect in the spinal cord (14), and P/Q-type VDCCs mediate interneuronal communication in the dorsal horn (12, 15). *Rolling mouse Nagoya*, a spontaneously occurring P/Q-type VDCC mutant mouse, has lowered sensitivity to nociceptive stimuli (16).

The participation of L-type VDCCs in nociceptive transmission depends on the type of pain (4). In the deep dorsal horn, persistent postsynaptic excitations such as the generation of plateau potentials (17, 18) and the induction of wind-up (18 – 20) are evoked by L-type VDCCs. Immunohistochemical studies have shown that two L-type VDCC subtypes each containing a distinct $\alpha 1$ subunit, $Ca_V1.2$ and $Ca_V1.3$, are expressed in the spinal cord (21, 22). $Ca_V1.2$ channels tend to be localized in somata and proximal dendrites, whereas $Ca_V1.3$ channels are present in somata and the whole dendritic region as far as distal dendrites (21, 23, 24). L-type VDCC-dependent wind-up occurs very similarly in both dorsal horn neuron discharges and motoneuronal flexion reflexes (19). Therefore it is considered that the activities of dorsal horn neurons are conveyed to the ventral horn motoneurons.

Our previous study using adult rats showed that after-discharges persisted for about 60 s in the ventral root after cessation of noxious mechanical stimuli (Fig. 1) (25). The after-discharges were inhibited by resiniferatoxin, which produced long-lasting desensitization of transient receptor potential channel TRPV1-positive afferents, and antagonists of nociceptive neurotransmitters (25). Therefore, it is considered that the after-discharges are derived from activation of C-fibers and subsequent persistent pain transduction in the spinal cord. In the present study, using each of these VDCC blockers, we examined whether spinal VDCCs contribute to the after-discharges evoked by mechanical nociception in adult rats. These channel blockers were applied directly to the spinal cord surface (Fig. 1A) to avoid any cardiovascular effects. As plateau potentials generated by L-type VDCCs are also observed in spinal motoneurons (26, 27), nicardipine, a selective L-type VDCC blocker, was injected directly into the dorsal and ventral horn to clarify the site of L-type VDCCs involved in the generation of after-discharges.

Materials and Methods

All experimental protocols used here were approved by the Animal Care and Use Committee of Nagoya City University and conducted in accordance with the *Guiding Principles for the Care and Use of Laboratory Animals* approved by The Japanese Pharmacological Society.

Surgery

This study was performed using 92 male Wistar/ST rats (7 – 9-week-old; SLC, Shizuoka). The animals were anesthetized with α-chloralose [150 mg/kg, intraperitoneally (i.p.)], and cannulae were then inserted into the trachea for artificial respiration (70/min, 1 ml/100 g body weight, end-tidal CO_2 concentration about 5%). To spinalize the rats, the vagus nerves were cut bilaterally in the cervical region to eliminate any parasympathomimetic effects on the heart, and the spinal cord was transected at the first cervical segmental (C1) level under lidocaine anesthesia (4%, 50 μl). A dorsal laminectomy was then performed in the lumbo-sacral region of each rat. On the L1 vertebra, an agar pool was created with 4% agar to facilitate application of drugs to the spinal surface (Fig. 1A), except in cases where drugs were injected into the spinal ventral and dorsal horns. Both the ventral and

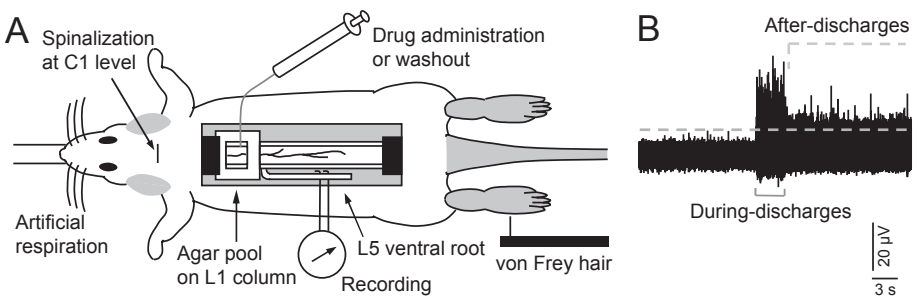

Fig. 1. Schematic representation of measurement of ventral root discharges. A: An overview of the anesthetized rat used in this study. Drug solution (50 μl) was applied by a microsyringe into an agar pool and suctioned by another syringe. Application and wash-out were done between stimuli. The left plantar surface of a hindpaw was mechanically stimulated for 3 s using a von Frey hair. B: Recorded L5 spinal ventral root discharges. The discharges in 3 s during the stimulation are defined as "during-discharges" and those 60 s after the stimulation as "after-discharges". These responses were normalized by subtraction of the spontaneous activity measured before application of the stimuli (dashed line).

dorsal roots below the sixth lumbar segment (L6) were cut distally at their points of exit from the vertebral column. The left fifth lumbar segmental (L5) ventral root was sectioned for recording, and the ipsilateral L5 dorsal root was left intact to receive peripheral signals. The entire exposed surgical area was covered with liquid paraffin that was maintained at 36°C ± 0.5°C by radiant heat. Rectal temperature was maintained at 36°C ± 0.5°C. Heart rate was monitored with needle electrodes inserted into both forepaws.

Measurement of ventral root discharges

The left plantar surface of a hindpaw was mechanically stimulated using a von Frey hair (75.9 g, Semmes-Weinstein monofilaments; Stoelting, Wood Dale, IL, USA). Each stimulus was applied for 3 s to the most sensitive point where the largest number of discharges was observed. The ventral root discharges occurring during the 3 s of stimulation were defined as "during-discharges" and those occurring during 60 s after the stimulation as "after-discharges". These responses were normalized by subtraction of the spontaneous activity measured before application of the stimuli (Fig. 1B). A pair of Ag–AgCl wire electrodes was used for recording. Motoneuronal multi-unit firing recorded from the left L5 whole ventral root was amplified and displayed on an oscilloscope (VC-10; Nihon Kohden, Tokyo). The signals were recorded on a DAT recorder (sampling rate: 40 kHz, PC-108M; Sony, Tokyo), and analyzed using a PowerLab (ADInstruments, Colorado Springs, CO, USA) and Chart software.

Drugs

α-Chloralose was obtained from Tokyo Kasei (Tokyo); ethosuximide, diltiazem HCl, and nicardipine HCl, from Sigma-Aldrich (St. Louis, MO, USA); verapamil HCl, from Wako Pure Chemical Industries (Osaka); and ω-conotoxin GVIA and ω-agatoxin IVA, from the Peptide Institute (Osaka). α-Chloralose, an anesthetic drug, was dissolved in distilled water and administered intraperitoneally. Other drugs were dissolved in saline and applied directly to the spinal cord in 50-μl volumes. Only ω-conotoxin GVIA and ω-agatoxin IVA were dissolved in saline containing 0.1 mg/ml cytochrome *c* to prevent non-specific peptide binding (12). Administration of each vehicle was performed in control groups.

Electrophysiology protocols

The testing protocol was application of von Frey stimuli every 10 min. Vehicle was applied to the agar pool on the spinal cord and three serial ventral root discharges were recorded to test whether these responses were stable. If the three serial responses were unstable, the vehicle application and three recordings were performed again. These three values were then averaged to generate pre-drug values (100%) with which to compare the effects of drug administration on subsequent evoked responses. The solution in the pool was washed out and replaced with a higher dose every 30 min (every three stimulations) except for ω-conotoxin GVIA and ω-agatoxin IVA, which were applied every 60 min because of the gradual appearance of their effects. In the control groups, vehicle was administrated at the each point instead of drugs. When nicardipine was used, the administration site was shaded with aluminum foil.

The method used for microinjection of drugs into the spinal cord was modified from Bell et al. (28) and Shimizu et al. (29). Two-barreled glass pipettes (1.5-mm outside diameter, GD-1.5; Narishige, Tokyo) were pulled using an electrode puller (PE-2, Narishige) and the tips were adjusted to 40 – 50 μm with the aid of a microscope. One barrel was filled with the drug solution and the other with dye (Brilliant Blue, 0.1 μl). One end of a polyethylene tube (30 cm, SP 31; Natsume, Tokyo) was glued to a glass micropipette and the other was connected to a 5-μl microsyringe (MS-05; Terumo, Tokyo). The glass micropipettes were inserted into the dorsal root entry zone between segments L4 and L5 (0.8 – 1.0 mm lateral to the midline). The micropipette tip was positioned at 0.45 mm and 1.5 mm below the pial surface for microinjection into the dorsal and ventral horn, respectively. The solution was injected slowly; 0.1 μl was injected over a period of 60 s. After the study, we injected dye into the dorsal and ventral horns of the spinal cord and confirmed that the dye stayed very close to the injection site.

Statistical analyses

All data were expressed as the mean ± S.E.M. Student's *t*-test was used to compare data for two groups. The paired *t*-test was used to compare heart rate data. Differences at $P < 0.05$ (two-tailed) were considered to be significant.

Results

In this study, drugs were applied directly to the spinal cord to avoid any cardiovascular effects. There were no significant differences in heart rate resulting from administration of vehicle alone and that resulting from administration of the highest doses of VDCC blockers (Table 1). The average firing rate before drug treatment of during-discharges was 271.9 ± 7.7 Hz (n = 92) and of after-discharges was 57.6 ± 2.8 Hz (n = 92).

Table 1. Comparison of heart rate between the presence of vehicle and after administration of the highest dose of VDCC blockers

VDCC blockers		Vehicle (bpm)	Highest dose (bpm)
Ethosuximide	(n = 6)	347 ± 9	354 ± 8
ω-Conotoxin GVIA	(n = 6)	370 ± 14	362 ± 11
ω-Agatoxin IVA	(n = 5)	370 ± 6	373 ± 4
Diltiazem	(n = 6)	328 ± 4	318 ± 2
Verapamil	(n = 6)	365 ± 10	366 ± 8
Nicardipine (i.t.)	(n = 6)	319 ± 15	321 ± 19
(intraspinal: dorsal horn)	(n = 6)	317 ± 6	318 ± 6
(intraspinal: ventral horn)	(n = 6)	316 ± 5	314 ± 6

Data are reported as the mean ± S.E.M.

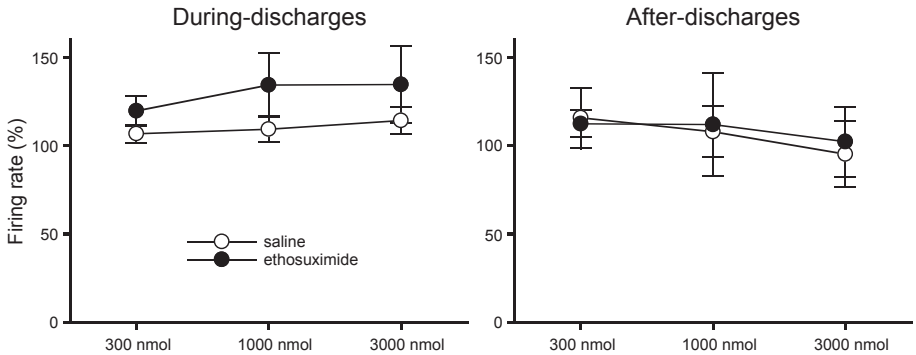

Fig. 2. Effects of ethosuximide (300, 1000, and 3000 nmol), a T-type VDCC blocker, applied directly to the surface of the spinal cord on during- and after-discharges. Three values were averaged to generate pre-drug values (100%) with which to compare the effect of ethosuximide on subsequent evoked responses. The solution in the pool was washed out and replaced by a higher dose every 3 responses. As a control group, 50 μl saline was administered instead of ethosuximide. The data represent the mean ± S.E.M. of 6 rats in each group.

Effects of T-type VDCC blocker on during- and after-discharges

The T-type VDCC blocker ethosuximide was applied directly to the spinal cord and the effect on ventral root discharges was examined (Fig. 2). Upon administration of 3000 nmol, during-discharges [control: 114.4% ± 7.5% (n = 6), 3000 nmol: 134.9% ± 21.5% (n = 6)] and after-discharges [control: 95.5% ± 19.0% (n = 6), 3000 nmol: 102.5% ± 19.8% (n = 6)] were not changed (Fig. 2).

Effects of N- and P/Q-type VDCC blockers on during- and after-discharges

Inhibition of N-type VDCCs with ω-conotoxin GVIA reduced the after-discharges (Fig. 3) at a low dose [control: 113.3% ± 10.9% (n = 6), 0.1 nmol: 64.9% ± 12.2% (n = 6), $P < 0.05$]. At the highest dose, during-discharges were inhibited [control: 100.1% ± 11.1% (n = 6), 1.0 nmol: 57.0% ± 10.3% (n = 6), $P < 0.05$] and after-discharges were markedly decreased [control: 86.0% ± 15.8% (n = 6), 1.0 nmol: 15.8% ± 7.0% (n = 6), $P < 0.01$]. On the other hand, the P/Q-type VDCC blocker ω-agatoxin IVA reduced the during- [control: 98.5 ± 8.6% (n = 5), 1.0 nmol: 48.9% ± 14.3% (n = 5), $P < 0.05$] and after- [control: 78.6 ± 10.8% (n = 5), 1.0 nmol: 26.0% ± 10.6% (n = 5), $P < 0.01$] discharges nonselectively in the high-dose group (Fig. 4).

Effects of L-type VDCC blockers on during- and after-discharges

Diltiazem HCl, an L-type VDCC blocker of the benzothiazepine class, reduced the during- [control: 122.0% ± 17.4% (n = 6), 300 nmol: 72.4% ± 8.5% (n = 6), $P < 0.05$] and after- [control: 135.2% ± 27.5% (n = 6), 300 nmol: 44.6% ± 8.4% (n = 6), $P < 0.05$] discharges nonselectively (Fig. 5A). In the high-dose (1000 nmol) group, after-discharges were largely diminished [3.3% ± 3.2% (n = 6)]. Verapamil HCl, an L-type VDCC blocker of the phenylalkylamine class, also reduced the during- [control: 101.1% ± 4.5% (n = 6), 300 nmol: 52.8% ± 11.3% (n = 6), $P < 0.01$] and after- [control:

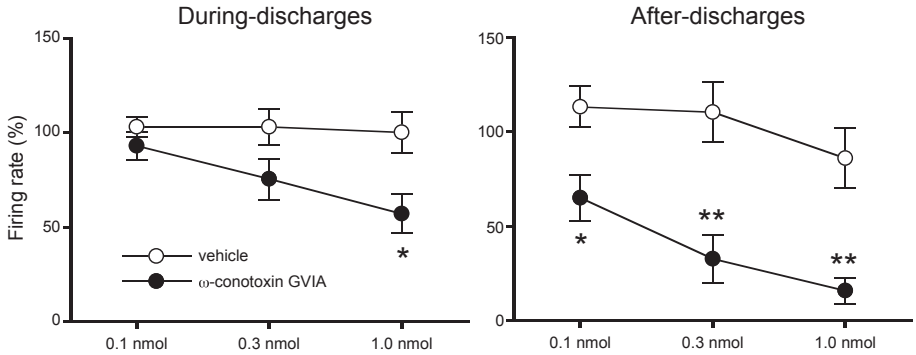

Fig. 3. Effects of ω-conotoxin GVIA (0.1, 0.3, and 1.0 nmol), an N-type VDCC blocker, applied directly to the surface of the spinal cord on during- and after-discharges. Three values after administration of vehicle were averaged to generate pre-drug values (100%) with which to compare the effect of ω-conotoxin GVIA on subsequent evoked responses. The solution in the pool was washed out and replaced by a higher dose every 6 responses. As a control group, 50 μl vehicle was administered instead of ω-conotoxin GVIA. The data represent the mean ± S.E.M. of 6 rats in each group. The statistical significance of differences was determined by Student's *t*-test. *$P < 0.05$, **$P < 0.01$ vs. vehicle.

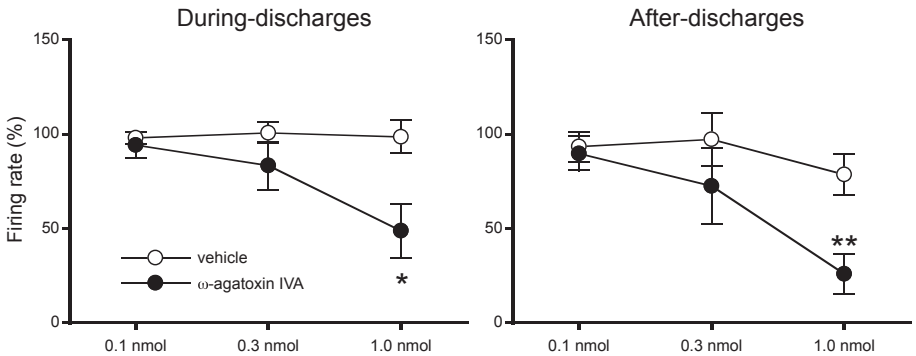

Fig. 4. Effects of ω-agatoxin IVA (0.1, 0.3, and 1.0 nmol), a P/Q-type VDCC blocker, applied directly to the surface of the spinal cord on during- and after-discharges. Three values after administration of vehicle were averaged to generate pre-drug values (100%) with which to compare the effect of ω-agatoxin IVA on subsequent evoked responses. The solution in the pool was washed out and replaced by a higher dose every 6 responses. As a control group, 50 μl vehicle was administered instead of ω-agatoxin IVA. The data represent the mean ± S.E.M. of 5 rats in each group. The statistical significance of differences was determined by Student's *t*-test. *$P < 0.05$, **$P < 0.01$ vs. vehicle.

95.0% ± 8.1% (n = 6), 300 nmol: 24.6% ± 11.0% (n = 6), $P < 0.01$] discharges nonselectively in the high-dose group (Fig. 5B).

On the other hand, selective reduction of after-discharges occurred upon administration of nicardipine at 300 nmol [control: 129.2% ± 17.1% (n = 6), 300 nmol: 40.4% ± 9.0% (n = 6), $P < 0.01$]. There were no significant differences in the during-discharges [control: 111.6% ± 9.1% (n = 6), 300 nmol: 84.4% ± 10.2% (n = 6)] (Fig. 6A).

To clarify the site of action of nicardipine, it was microinjected into the spinal dorsal or ventral horn (Fig. 6B). Ventral horn injection of nicardipine at 0.1 nmol influenced neither during-discharges [control: 118.7% ± 6.4% (n = 5), 0.1 nmol: 103.2% ± 8.4% (n = 6)] nor after-discharges [control: 143.8% ± 19.3% (n = 5), 0.1 nmol: 110.8% ± 12.1% (n = 6)]. Dorsal horn injection selectively suppressed after-discharges [control: 103.9% ± 7.6% (n = 5), 0.1 nmol: 74.7% ± 4.4% (n = 6), $P < 0.01$] but not during-discharges [control: 96.9% ± 3.1% (n = 5), 0.1 nmol: 101.5% ± 2.1% (n = 6)].

Discussion

Noxious mechanical stimuli applied to the plantar surface of the foot evoked during- and after-discharges at the corresponding ventral root L5 (Fig. 1) (25). Touch, pressure, and noxious stimuli produced during-discharges and noxious stimulation using a strong von Frey hair (75.9 g) produced after-discharges (25). To explore the involvement of VDCCs in these ventral root discharges, several VDCC blockers were applied directly to the spi-

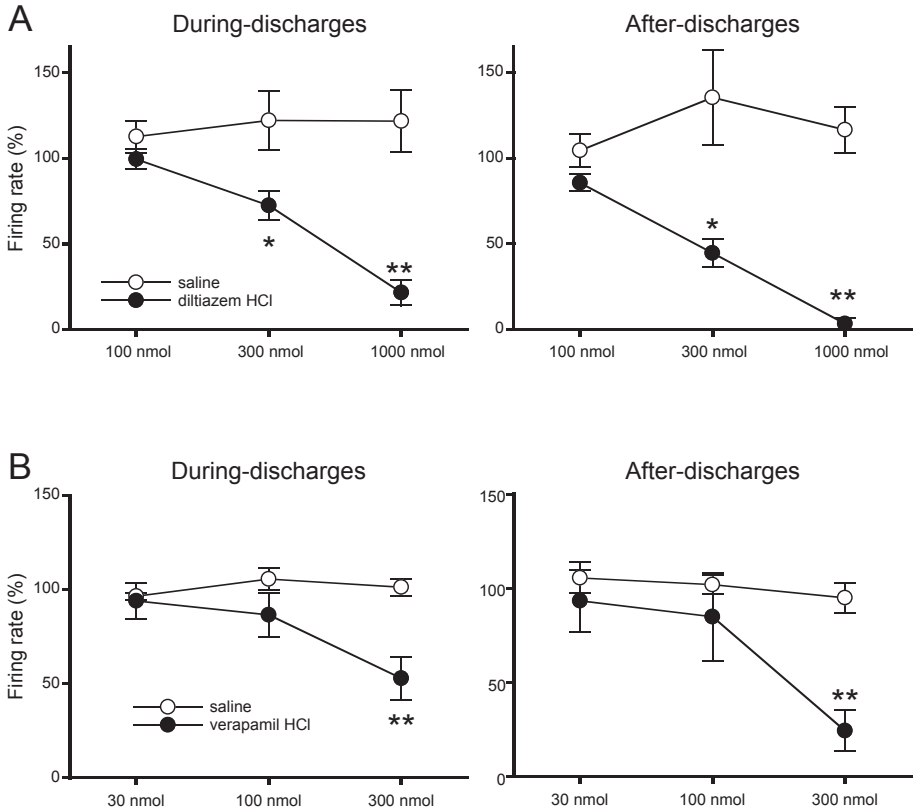

Fig. 5. Effects of diltiazem (A: 100, 300, and 1000 nmol) and verapamil (B: 30, 100, and 300 nmol), L-type VDCC blockers, applied directly to the surface of the spinal cord on during- and after-discharges. Three values after administration of saline were averaged to generate pre-drug values (100%) with which to compare the effects of the drugs on subsequent evoked responses. The solution in the pool was washed out and replaced by a higher dose every 3 responses. As a control group, 50 μl saline was administered instead of drugs. The data represent the mean ± S.E.M. of 6 rats in each group. The statistical significance of differences was determined by Student's *t*-test. $*P < 0.05$, $**P < 0.01$ vs. vehicle.

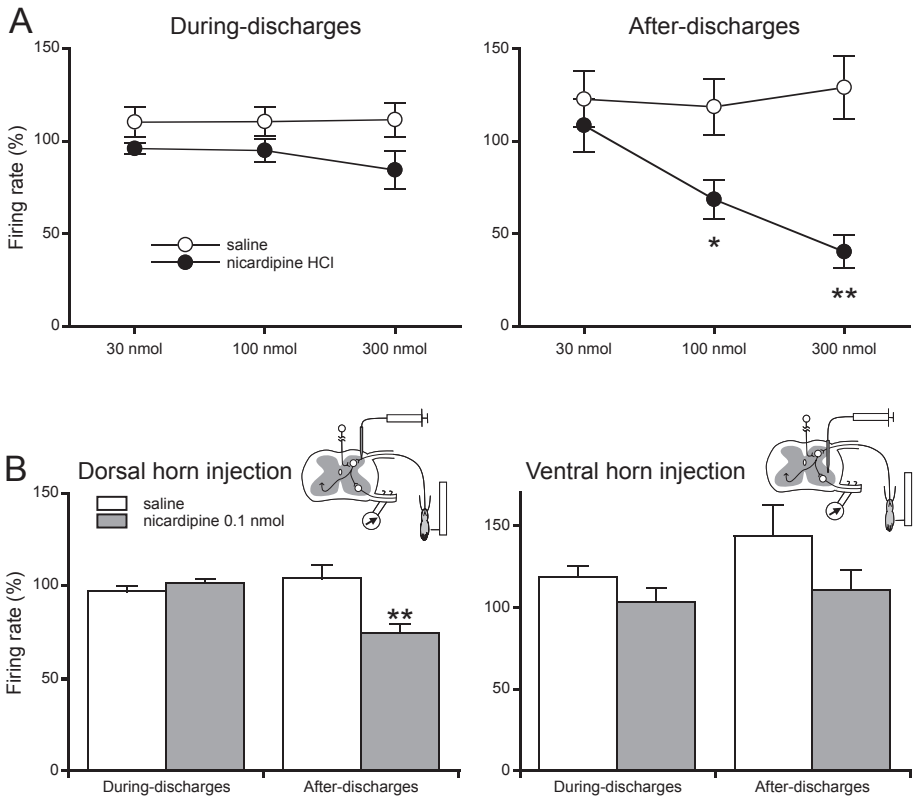

Fig. 6. Effects of nicardipine, an L-type VDCC blocker, applied directly to the surface of the spinal cord (A: 30, 100, and 300 nmol) and into the dorsal or ventral horn (B: 0.1 nmol), on during- and after-discharges. Insets in panel B show schematic representations of the microinjection into the dorsal and ventral horn, respectively. Three values after administration of saline were averaged to generate pre-drug values (100%) with which to compare the effects of the drug on subsequent evoked responses. As a control group, 50 μl (A) or 0.1 μl (B) saline was administered instead of nicardipine. The data represent the mean ± S.E.M. of 5 – 6 rats in each group. The statistical significance of differences was determined by Student's *t*-test. $*P < 0.05$, $**P < 0.01$ vs. saline.

nal cord surface. Ethosuximide (a T-type VDCC blocker) had no effect on the ventral root discharges (Fig. 2). ω-Conotoxin GVIA (an N-type VDCC blocker) showed preferential suppression of after-discharges (Fig. 3), and ω-agatoxin IVA (a P/Q-type VDCC blocker) nonselectively depressed both during- and after-discharges at high dose (Fig. 4). Diltiazem and verapamil, L-type VDCC blockers, also displayed nonselective depression of both ventral root discharges (Fig. 5). The more selective L-type VDCC blocker nicardipine depressed only after-discharges (Fig. 6A), and depression was evident when nicardipine was injected into the dorsal horn, but not into the ventral horn (Fig. 6B). These findings suggested that N- and L-type VDCCs in the dorsal horn were involved in the generation of after-discharges.

The T-type VDCC blocker ethosuximide did not influence during- or after-discharges (Fig. 2). Several studies have identified T-type VDCCs in small- and medium-sized neurons of dorsal root ganglion (DRG) (3) and have shown that they are important in peripheral processing of noxious signals (30, 31). Since T-type VDCCs are critical mediators of the excitability of primary afferent fibers (6), it may have been difficult to observe the inhibitory effect of ethosuximide in the present study using the spinal cord. Intrathecal administration of ethosuximide also does not affect the formalin test in both phases (32), but has been shown to inhibit dorsal horn neuronal responses evoked by natural stimuli in an in vivo electrophysiological study (14). Although it is considered that the dose used in the present study was sufficient to block the T-type Ca^{2+} current (33), the precise function of T-type VDCCs in the complex spinal dorsal horn circuitry remains unclear.

ω-Conotoxin GVIA showed more preferential inhibition of after-discharges than during-discharges (Fig. 3). ω-Conotoxin GVIA has been shown to produce irreversible blockade of N-type VDCCs (34), both presynaptically (11) and postsynaptically (12), in lamina I. Therefore, it seems that the inhibition of after-discharges by ω-conotoxin GVIA was attributable to reduced noxious inputs to the dorsal horn. The effect of ω-conotoxin GVIA on after-discharges was similar to that of morphine and a neurokinin 1–receptor antagonist, respectively, administered intravenously (25). These results are supported by studies indicating that N-type VDCCs were inhibited by μ-opioid receptors in the DRG (35, 36) and that N-type VDCC blockers inhibited the release of substance P in the spinal cord (8, 37, 38).

Unlike ω-conotoxin GVIA, ω-agatoxin IVA exhibited similar attenuation of both during- and after-discharges (Fig. 4). P/Q-type VDCC blockers contribute less than N-type VDCCs to the voltage-gated Ca^{2+} current in the DRG (39) and have no effect on the input from primary afferent fibers into dorsal horn neurons (5, 34). Although both N- and P/Q-type VDCCs are expressed in the spinal cord, P/Q-type VDCCs are localized primarily in interneurons (15). P/Q-type VDCC blockers also suppress polysynaptic transmission (12). This inhibitory action on polysynaptic transmission may be represented as inhibition of during- and after-discharges.

Three L-type VDCC blockers were used to confirm the contribution of L-type VDCCs to ventral root discharges. Diltiazem and verapamil exerted an inhibitory influence on both during- and after-discharges (Fig. 5), whereas nicardipine showed a selective effect on after-discharges (Fig. 6). Although diltiazem HCl and verapamil HCl are known to be water-soluble L-type VDCC blockers, they also inhibit P/Q- and R-type VDCCs at the same doses in L-type VDCCs (40, 41). These effects reconfirmed that inhibition of P/Q-type VDCCs contributed to the reduction of both during- and after-discharges, coincident with the effect of ω-agatoxin IVA (Fig. 4). The inhibitory action of high-dose diltiazem and verapamil on Na^+ channels (41) also lends support to the inhibition of ventral root discharges via blockage of action potentials in the spinal cord. Nicardipine has been shown to block not only L-type but also other VDCCs, but has higher affinity for L-type VDCCs than for N- and P/Q-type VDCCs (42, 43). T-type VDCCs (44) probably did not participate in the blocking effect of nicardipine on ventral root discharges because ethosuximide did not reduce the discharges (Fig. 2). The blocking effects of nicardipine on glycine and $GABA_A$ receptors (45) and the K^+ channel (46) would also be unrelated because blockage of these channels enhanced the neuronal output. These findings suggest that the inhibitory effect of nicardipine on after-discharges occurs through blockade of L-type VDCCs.

A plateau potential involved in sustained depolarization evoked by nociceptive inputs is observed in deep dorsal horn neurons (17, 18). It is considered that this plateau potential is one of the mechanisms responsible for generation of after-discharges (47) caused by L-type VDCCs (17, 18). Therefore it appears that the generation of after-discharges was inhibited by blockade of L-type VDCCs by nicardipine. Two types of L-type VDCC α-subunits, $Ca_V1.2$ and $Ca_V1.3$, are expressed in the spinal cord (21, 22). $Ca_V1.3$-containing channels have a much lower activation threshold than $Ca_V1.2$ channels and are preferentially involved in genesis of the plateau potential (26, 48). Although $Ca_V1.3$-containing channels are 10 – 20 times less sensitive to dihydropyridine than $Ca_V1.2$ channels (49), nicardipine showed a selective effect on after-discharges (Fig. 6A). The dose of nicardipine used in this study was thought to be enough for inhibition of after-discharges.

$Ca_V1.3$ are expressed not only in the spinal dorsal horn (21) but also the ventral horn (24, 48) and contribute to the generation of plateau potentials in motoneurons (26, 50). However during- and after-discharges were not inhibited by injection of nicardipine into the spinal cord ventral horn (Fig. 6B). Therefore it was confirmed that the effect of nicardipine applied to the superficial spinal cord is not due to diffusion of the drug to the ventral horn. After-discharges were affected to the same degree by nicardipine at 100 nmol applied to the spinal surface (Fig. 6A) and 0.1 nmol injected into the ventral horn (Fig. 6B). This difference in the dose effect was considered attributable to partial penetration of nicardipine from the spinal surface. On the other hand, microinjection of nicardipine into the spinal dorsal horn as well as its superficial application to the spinal cord attenuated after-discharges. This result suggests that the site of action of nicardipine applied directly to the spinal cord surface is the dorsal horn. Thus, it was considered that after-discharges were generated in the dorsal horn and transmitted to motoneurons in the ventral horn in a manner analogous to wind-up of a nociceptive flexion reflex (19).

In conclusion, the findings of this study suggest that N- and L-type VDCCs play an important role in the ventral root after-discharges evoked by nociceptive mechanical stimuli applied to the hindpaw. The distribution and function of these channels in the spinal cord suggest that N-type VDCCs are involved in the presynaptic component including primary afferent fibers, whereas L-type VDCCs are involved in the postsynaptic component including dorsal horn neurons, both of which contribute to persistent nociceptive transmission in the spinal cord. Blockers of both N- and L-type VDCC such as cilnidipine (51, 52) and amlodipine (53) may be useful for treatment of persistent pain involving the spinal pathway.

Acknowledgment

This work was supported by a Grant-in-Aid for Research at Nagoya City University.

References

1 Vacher H, Mohapatra DP, Trimmer JS. Localization and targeting of voltage-dependent ion channels in mammalian central neurons. Physiol Rev. 2008;88:1407–1447.
2 Carlin KP, Jiang Z, Brownstone RM. Characterization of calcium currents in functionally mature mouse spinal motoneurons. Eur J Neurosci. 2000;12:1624–1634.
3 Talley EM, Cribbs LL, Lee JH, Daud A, Perez-Reyes E, Bayliss DA. Differential distribution of three members of a gene family encoding low voltage-activated (T-type) calcium channels. J Neurosci. 1999;19:1895–1911.
4 Vanegas H, Schaible H. Effects of antagonists to high-threshold calcium channels upon spinal mechanisms of pain, hyperalgesia and allodynia. Pain. 2000;85:9–18.
5 Ohnami S, Tanabe M, Shinohara S, Takasu K, Kato A, Ono H. Role of voltage-dependent calcium channel subtypes in spinal long-term potentiation of C-fiber-evoked field potentials. Pain. 2011;152:623–631.
6 Zamponi GW, Lewis RJ, Todorovic SM, Arneric SP, Snutch TP. Role of voltage-gated calcium channels in ascending pain pathways. Brain Res Rev. 2009;60:84–89.
7 Kim C, Jun K, Lee T, Kim SS, McEnery MW, Chin H, et al. Altered nociceptive response in mice deficient in the α_{1B} subunit of the voltage-dependent calcium channel. Mol Cell Neurosci. 2001;18:235–245.
8 Rycroft BK, Vikman KS, Christie MJ. Inflammation reduces the contribution of N-type calcium channels to primary afferent synaptic transmission onto NK1 receptor-positive lamina I neurons in the rat dorsal horn. J Physiol. 2007;580:883–894.
9 Weber AM, Wong FK, Tufford AR, Schlichter LC, Matveev V, Stanley EF. N-type Ca^{2+} channels carry the largest current: implications for nanodomains and transmitter release. Nat Neurosci. 2010;13:1348–1350.
10 Schmidtko A, Lötsch J, Freynhagen R, Geisslinger G. Ziconotide for treatment of severe chronic pain. Lancet. 2010;375:1569–1577.
11 Gruner W, Silva LR. ω-Conotoxin sensitivity and presynaptic inhibition of glutamatergic sensory neurotransmission *in vitro*. J Neurosci. 1994;14:2800–2808.
12 Heinke B, Balzer E, Sandkühler J. Pre- and postsynaptic contributions of voltage-dependent Ca^{2+} channels to nociceptive transmission in rat spinal lamina I neurons. Eur J Neurosci. 2004;19:103–111.
13 Maeda Y, Aoki Y, Sekiguchi F, Matsunami M, Takahashi T, Nishikawa H, et al. Hyperalgesia induced by spinal and peripheral hydrogen sulfide: evidence for involvement of $Ca_V3.2$ T-type calcium channels. Pain. 2009;142:127–132.
14 Matthews EA, Dickenson AH. Effects of ethosuximide, a T-type Ca^{2+} channel blocker, on dorsal horn neuronal responses in rats. Eur J Pharmacol. 2001;415:141–149.
15 Mintz IM, Adams ME, Bean BP. P-type calcium channels in rat central and peripheral neurons. Neuron. 1992;9:85–95.
16 Fukumoto N, Obama Y, Kitamura N, Niimi K, Takahashi E, Itakura C, et al. Hypoalgesic behaviors of P/Q-type voltage-gated Ca^{2+} channel mutant mouse, *rolling mouse Nagoya*. Neuroscience. 2009;160:165–173.
17 Voisin DL, Nagy F. Sustained L-type calcium currents in dissociated deep dorsal horn neurons of the rat: characteristics and modulation. Neuroscience. 2001;102:461–472.
18 Morisset V, Nagy F. Plateau potential-dependent windup of the response to primary afferent stimuli in rat dorsal horn neurons. Eur J Neurosci. 2000;12:3087–3095.
19 Fossat P, Sibon I, Le MG, Landry M, Nagy F. L-type calcium channels and NMDA receptors: a determinant duo for short-term nociceptive plasticity. Eur J Neurosci. 2007;25:127–135.
20 Russo RE, Hounsgaard J. Short-term plasticity in turtle dorsal horn neurons mediated by L-type Ca^{2+} channels. Neuroscience. 1994;61:191–197.
21 Dobremez E, Bouali-Benazzouz R, Fossat P, Monteils L, Dulluc J, Nagy F, et al. Distribution and regulation of L-type calcium channels in deep dorsal horn neurons after sciatic nerve injury in

rats. Eur J Neurosci. 2005;21:3321–3333.
22 Murakami M, Nakagawasai O, Suzuki T, Mobarakeh II, Sakurada Y, Murata A, et al. Antinociceptive effect of different types of calcium channel inhibitors and the distribution of various calcium channel α_1 subunits in the dorsal horn of spinal cord in mice. Brain Res. 2004;1024:122–129.
23 Jiang Z, Rempel J, Li J, Sawchuk MA, Carlin KP, Brownstone RM. Development of L-type calcium channels and nifedipine-sensitive motor activity in the postnatal mouse spinal cord. Eur J Neurosci. 1999;11:3481–3487.
24 Zhang M, Sukiasyan N, Møller M, Bezprozvanny I, Zhang H, Wienecke J, et al. Localization of L-type calcium channel $Ca_V1.3$ in cat lumbar spinal cord--with emphasis on motoneurons. Neurosci Lett. 2006;407:42–47.
25 Yamamoto S, Honda M, Tanabe M, Ono H. Spinal ventral root after-discharges as a pain index: involvement of NK-1 and NMDA receptors. Brain Res. 2006;1082:115–123.
26 Alaburda A, Perrier JF, Hounsgaard J. Mechanisms causing plateau potentials in spinal motoneurones. Adv Exp Med Biol. 2002;508:219–226.
27 Booth V, Rinzel J, Kiehn O. Compartmental model of vertebrate motoneurons for Ca^{2+}-dependent spiking and plateau potentials under pharmacological treatment. J Neurophysiol. 1997;78: 3371–3385.
28 Bell JA, Sharpe LG, Berry JN. Depressant and excitant effects of intraspinal microinjections of morphine and methionine-enkephalin in the cat. Brain Res. 1980;196:455–465.
29 Shimizu S, Honda M, Tanabe M, Ono H. $GABA_B$ receptors do not mediate the inhibitory actions of gabapentin on the spinal reflex in rats. J Pharmacol Sci. 2004;96:444–449.
30 Choi S, Na HS, Kim J, Lee J, Lee S, Kim D, et al. Attenuated pain responses in mice lacking $Ca_V3.2$ T-type channels. Genes Brain Behav. 2007;6:425–431.
31 Todorovic SM, Meyenburg A, Jevtovic-Todorovic V. Mechanical and thermal antinociception in rats following systemic administration of mibefradil, a T-type calcium channel blocker. Brain Res. 2002;951:336–340.
32 Cheng JK, Lin CS, Chen CC, Yang JR, Chiou LC. Effects of intrathecal injection of T-type calcium channel blockers in the rat formalin test. Behav Pharmacol. 2007;18:1–8.
33 Todorovic SM, Lingle CJ. Pharmacological properties of T-type Ca^{2+} current in adult rat sensory neurons: effects of anticonvulsant and anesthetic agents. J Neurophysiol. 1998;79:240–252.
34 Motin L, Adams DJ. ω-Conotoxin inhibition of excitatory synaptic transmission evoked by dorsal root stimulation in rat superficial dorsal horn. Neuropharmacology. 2008;55:860–864.
35 Andrade A, Denome S, Jiang YQ, Marangoudakis S, Lipscombe D. Opioid inhibition of N-type Ca^{2+} channels and spinal analgesia couple to alternative splicing. Nat Neurosci. 2010;13:1249–1256.
36 Wu ZZ, Chen SR, Pan HL. Differential sensitivity of N- and P/Q-type Ca^{2+} channel currents to a μ opioid in isolectin B_4-positive and -negative dorsal root ganglion neurons. J Pharmacol Exp Ther. 2004;311:939–947.
37 Smith MT, Cabot PJ, Ross FB, Robertson AD, Lewis RJ. The novel N-type calcium channel blocker, AM336, produces potent dose-dependent antinociception after intrathecal dosing in rats and inhibits substance P release in rat spinal cord slices. Pain. 2002;96:119–127.
38 Takasusuki T, Yaksh TL. Regulation of spinal substance p release by intrathecal calcium channel blockade. Anesthesiology. 2011; 115:153–164.
39 McCallum JB, Wu HE, Tang Q, Kwok WM, Hogan QH. Subtype-specific reduction of voltage-gated calcium current in medium-sized dorsal root ganglion neurons after painful peripheral nerve injury. Neuroscience. 2011;179:244–255.
40 Cai D, Mulle JG, Yue DT. Inhibition of recombinant Ca^{2+} channels by benzothiazepines and phenylalkylamines: class-specific pharmacology and underlying molecular determinants. Mol Pharmacol. 1997;51:872–881.
41 Martinez-Gomez J, Lopez-Garcia JA. Simultaneous assessment of the effects of L-type current modulators on sensory and motor pathways of the mouse spinal cord in vitro. Neuropharmacology. 2007;53:464–471.
42 Diochot S, Richard S, Baldy-Moulinier M, Nargeot J, Valmier J. Dihydropyridines, phenylalkylamines and benzothiazepines block N-, P/Q- and R-type calcium currents. Pflugers Arch. 1995;431:10–19.
43 Furukawa T, Yamakawa T, Midera T, Sagawa T, Mori Y, Nukada T. Selectivities of dihydropyridine derivatives in blocking Ca^{2+} channel subtypes expressed in *Xenopus* oocytes. J Pharmacol Exp Ther. 1999;291:464–473.
44 Furukawa T, Nukada T, Namiki Y, Miyashita Y, Hatsuno K, Ueno Y, et al. Five different profiles of dihydropyridines in blocking T-type Ca^{2+} channel subtypes ($Ca_v3.1$ (α_{1G}), $Ca_v3.2$ (α_{1H}), and $Ca_v3.3$ (α_{1I})) expressed in *Xenopus oocytes*. Eur J Pharmacol. 2009;613:100–107.
45 Chesnoy-Marchais D, Cathala L. Modulation of glycine responses by dihydropyridines and verapamil in rat spinal neurons. Eur J Neurosci. 2001;13:2195–2204.
46 Hatano N, Ohya S, Muraki K, Giles W, Imaizumi Y. Dihydropyridine Ca^{2+} channel antagonists and agonists block Kv4.2, Kv4.3 and Kv1.4 K^+ channels expressed in HEK293 cells. Br J Pharmacol. 2003;139:533–544.
47 Morisset V, Nagy F. Nociceptive integration in the rat spinal cord: role of non-linear membrane properties of deep dorsal horn neurons. Eur J Neurosci. 1998;10:3642–3652.
48 Simon M, Perrier JF, Hounsgaard J. Subcellular distribution of L-type Ca^{2+} channels responsible for plateau potentials in motoneurons from the lumbar spinal cord of the turtle. Eur J Neurosci. 2003;18:258–266.
49 Xu W, Lipscombe D. Neuronal $Ca_V1.3\alpha_1$ L-type channels activate at relatively hyperpolarized membrane potentials and are incompletely inhibited by dihydropyridines. J Neurosci. 2001;21: 5944–5951.
50 Elbasiouny SM, Bennett DJ, Mushahwar VK. Simulation of dendritic $Ca_V1.3$ channels in cat lumbar motoneurons: spatial distribution. J Neurophysiol. 2005;94:3961–3974.
51 Koganei H, Shoji M, Iwata S. Suppression of formalin-induced nociception by cilnidipine, a voltage-dependent calcium channel blocker. Biol Pharm Bull. 2009;32:1695–1700.
52 Murakami M, Nakagawasai O, Fujii S, Hosono M, Hozumi S, Esashi A, et al. Antinociceptive effect of cilnidipine, a novel N-type calcium channel antagonist. Brain Res. 2000;868:123–127.
53 Murakami M, Nakagawasai O, Fujii S, Kameyama K, Murakami S, Hozumi S, et al. Antinociceptive action of amlodipine blocking N-type Ca^{2+} channels at the primary afferent neurons in mice. Eur J Pharmacol. 2001;419:175–181.